



Original Research Article

CircZCCHC2 (hsa_circ_0000854) promotes hepatocellular carcinoma progression through modulating miR-936/BTBD7 axis and activating Rho/ROCK2 pathway

Junjie Yin ^{a,1}, Mian Wang ^{b,1}, Jian Chen ^a, Huigang Li ^a, Jianyong Zhuo ^a, Bei Lu ^a, Yang Cai ^{a,*}

^a Department of Hepatobiliary and Pancreatic Surgery, Affiliated Hangzhou First People's Hospital, School of medicine, Westlake university, Hangzhou, 310006, China

^b Department of Geriatric, Zhejiang Hospital of Integrated Traditional Chinese and Western Medicine, Hangzhou, 310003, China

ARTICLE INFO

Keywords:

Hepatocellular carcinoma
circZCCHC2
miR-936/BTBD7 axis
Tumorigenesis
Metastasis

ABSTRACT

Hepatocellular carcinoma (HCC) is one of the most aggressive and refractory cancers due to its high propensity to metastasize and the unavailability of efficacious treatments. Circular RNAs (circRNAs) participate in diverse biological activities in human cancers. Here, we detected the upregulation of a novel circRNA, circZCCHC2 (hsa_circ_0000854), in HCC samples and cells. The upregulation indicated an unfavorable prognosis in HCC patients. CircZCCHC2 accelerated cell growth and metastasis *in vitro* and tumorigenicity *in vivo*. Mechanistic investigations revealed that circZCCHC2 regulated BTBD7 expression by sponging miR-936. Moreover, the suppression of malignancy caused by circZCCHC2 knockdown could be sufficiently reversed by miR-936 inhibition. Additionally, the suppressed Rho/ROCK2 pathway conferred by circZCCHC2 knockdown could be restored by inhibiting miR-936 expression. Collectively, our findings reveal that circZCCHC2 plays an oncogenic role of in HCC progression by modulating the miR-936/BTBD7/Rho/ROCK2 pathway.

1. Introduction

Hepatocellular carcinoma (HCC) represents the most challenging subtype of primary liver tumor due to its increasing prevalence worldwide [1]. Globally, HCC ranks sixth among diagnosed cancers and fourth in mortality rates [2]. Chronic hepatitis B or C virus (HBV or HCV) infection, alcohol addiction, and nonalcoholic fatty liver disease are well-proven epidemiological risk factors for HCC [3,4]. In China, chronic HBV or HCV infection is the major cause of HCC cases [5]. Due to tumor heterogeneity and the lack of early diagnostic biomarkers and specific therapeutic targets, a considerable number of the HCC patients are diagnosed at an advanced stage and fail to receive timely treatment [6]. Therefore, identification of novel molecular targets with high specificity and sensitivity for HCC diagnosis and treatments is urgently needed.

Recently, circular RNAs (circRNAs) have been considered a new class of noncoding RNA and many circRNAs have been observed to be dysregulated in human cancers. CircRNAs are more resistant to RNA exonuclease due to the covalently closed loop structures, therefore more stable than linear non-coding RNAs. CircRNAs have been implicated in a

variety of cellular processes in human cancers, such as tumorigenesis, progression, relapse, metastasis, and drug resistance. For example, circRNA-SORE is upregulated in HCC cells and contributes to sorafenib resistance by suppressing PRP19-mediated YBX1 degradation [7]. The exosomal circRNA-100 is overexpressed in highly metastatic HCC cells, promoting the metastatic potential of HCC by regulating proangiogenic activity [8]. Additionally, hsa_circ_104348 facilitates HCC progression by modulating the miR-187-3p/RTKN2 axis and activating the Wnt/ β -catenin pathway [9]. In contrast, circRNA-5692 exerts anticarcinogenic effects in HCC by promoting DAB2IP expression [10].

Typically, circRNAs regulate gene expression by sponging of microRNAs (miRNAs), thus regulating the occurrence and development of malignancies [11]. CircMET has been found to sponge miR-30-5p to activate the Snail/DPP4/CXCL10 axis, thereby driving immunosuppression, thereby leading to the resistance of *anti*-PD1 therapy in HCC patients [12]. By contrast, hsa_circ_0001445 is decreased in HCC patients, which is positively correlated with the aggressive behaviors of HCC tumors. Moreover, cSMARCA5 functions as sponges of miR-17-3p and miR-181b-5p to upregulate TIMP3, a well-known tumor suppressor, thus inhibiting HCC malignancy [13]. Hence, circRNA can play either a

* Corresponding author.

E-mail address: caiyang6969@163.com (Y. Cai).

¹ Contributed equally to this work.

carcinogenic or an anticarcinogenic role in hepatocellular carcinoma. CircZCCHC2 is a novel discovering circRNA, which is formed from exons 2 to 5 of ZCCHC2. But the biogenesis processes, potential functions as well as precise mechanisms of circZCCHC2 in HCC tumorigenesis remains not fully understand.

Here, we investigated the roles of circZCCHC2 in HCC development and progression. Our data demonstrate that circZCCHC2 acts as a novel cancer-promoting gene in HCC cells. Silencing circZCCHC2 severely attenuates HCC progression both *in vitro* and *in vivo*. Mechanistically, circZCCHC2 can sponge miR-936 to upregulate BTBD7 and the activate Rho/ROCK2 signaling pathway in HCC cells.

2. Materials and methods

2.1. Human tissues

HCC samples and corresponding normal tissues were collected from the HCC patients who underwent surgery at the Affiliated Hangzhou First People's Hospital. None of the patients had received chemotherapy, radiotherapy, or targeted therapy prior to surgery. All experiments were approved by the Research Ethics Committee of the *Affiliated Hangzhou First People's Hospital* and were performed in accordance with the ethical guidelines of the Declaration of Helsinki.

2.2. Cell culture

Four human hepatocellular carcinoma cell lines (Hep3B, SK-HEP-1 HepG2, and Huh7) and a human normal hepatocyte (LO2) were obtained from the Bank of ATCC (Shanghai, China). The cells were cultured in high-glucose DMEM or 1640 media supplemented with 10 % FBS and grew in a 5 % CO₂ incubator at 37 °C.

2.3. DNA constructs, cell transfection, and viral transduction

The short hairpin RNA (shRNA) sequences of circZCCHC2 (sh-circZCCHC2#1 and sh-circZCCHC2#2) were designed and synthesized in Genechem (Shanghai, China). HEK293T cells were transfected with individual lentiviral vectors along with packaging plasmids to generate lentivirus stably expressing sh-circZCCHC2. After transfection for 48h, the lentivirus in the cell supernatant were filtered to infect target cells with polybrene (8 mg/mL).

Negative control of miRNA (miR-NC), miR-936 inhibitors, and miR-936 mimics were designed and synthesized in Genechem. Plasmids for expressing wild-type and mutant BTBD7 (BTBD7-WT and BTBD7-Mut) were synthesized in GenePharma (Shanghai, China) and verified by Sanger sequencing (Sangon Biotech). Transient transfection was performed using Lipofectamine 2000 (Invitrogen, #2041726). The efficiency of gene overexpression or silencing was validated by RT-qPCR analysis.

2.4. RNA extraction and RT-qPCR

RNA was extracted from cultured cells or tissues using TRIzol reagent (Takara, # 9109), and cDNA was synthesized using Hifair III Reverse Transcriptase (Yeasen, #11297ES75). Relative gene expression was calculated by normalization to the expression levels of GAPDH or U6. The primers for RT-qPCR were synthesized by HuaGene Biotech.

2.5. RNase R treatment

For the RNase R assay, a total of 10 µg RNA was treated by RNase R with incubation for 30 min at 37 °C, negative control (mock) was used to compare. Then the circZCCHC2 and ZCCHC2 mRNA was evaluated using qRT-PCR. The stability of linear ZCCHC2 mRNA and circZCCHC2 were compared by quantifying the RNA levels using RT-qPCR after treatment with 2 µg/mL of actinomycin D for 0, 6, 12, and 24 h at 37 °C.

2.6. Cell proliferation and EdU assays

For the cell viability assay, 1×10^3 Hep3B and HepG2 cells were seeded in 96-well plates. Cell growth curve was assessed using the CCK-8 kit (Yeasen, #40203ES92). For colony formation assays, 1.5×10^3 Hep3B and HepG2 cells were seeded in 6-well plates, and changed the medium every three days. After 10–14 days, the colonies were stained using crystal violet, and counted using Image J.

For the EdU assay, Hep3B and HepG2 cells were seeded in 96-well plates. Then the cells were fixed, permeated, and stained by the solution in the Light EdU Apollo Assay Kit (Ribobio, #C10310). Cell nuclei was stained using the Mounting Medium with DAPI (Abcam, #ab104139). The Leica SP5 fluorescence confocal microscope was used to image.

2.7. Cell migration and invasion assays

To assess cell migrative ability, 4×10^4 Hep3B and HepG2 cells resuspended FBS-free media were placed in the upper chamber without Matrigel (Corning Falcon, #353097). To explore cell invasive ability, 1×10^4 Hep3B and HepG2 cells resuspended in FBS-free media were seeded in the upper chamber with Matrigel (Corning BioCoat, #354480). For both cell migration and invasion assays, 800 µl of medium supplemented with 10 % FBS was added into the 24-well plates. After 20–24 h, the cells in the lower chamber were stained with crystal violet, imaged under a microscope, and counted using Image J.

2.8. Online analysis

The Gene Expression Omnibus (GEO) dataset, GES164803, was downloaded to analyze the differentially expressed circRNAs in six pairs of HCC specimens and corresponding normal tissues. The computational tool Circular RNA Interactome was used to predict and map the binding sequences of miR-936 and circZCCHC2. The MiRNA Target Prediction Database was utilized to predict and map the complementary sequences of miR-936 and BTBD7.

2.9. FISH assay

The probes of circZCCHC2 were purchased in GenePharma (Shanghai, China). To define the subcellular organelle localization of circZFR, the FISH assay was performed using a fluorescent *in situ* hybridization kit (Bersinbio, #Bes1002). The Leica SP5 fluorescence confocal microscope was used to image.

2.10. Luciferase reporter assay

To perform the luciferase reporter assay, circZCCHC2 containing the predicted miR-936 binding site and circZCCHC2 mutant containing point mutations of the miR-936 complementary sequence were cloned into the psiCHECK2 vectors (Promega, USA). To confirm the binding sequences between miR-936 and BTBD7, wild-type or mutant BTBD7 reporter was cloned into the psiCHECK2 Dual-luciferase (Promega, USA). Subsequently, the miR-936 mimics or negative control was co-transfected with either of the reporter plasmids (circZCCHC2 WT, circZCCHC2 MUT, BTBD7 WT, or BTBD7 MUT) into Hep3B and HepG2 cells. The luciferase activity was tested using Dual-Luciferase Reporter Gene Assay Kit (Yeasen, #11402ES60).

2.11. RNA-RNA pulldown assay

Biotinylated probes were purchased in Genepharma. For RNA pulldown assay, the probes were incubated with prewashed streptavidin-agarose beads (Thermo Scientific, USA). Then lysates of Hep3B and HepG2 cells were mixed fully with the streptavidin-agarose beads to generate RNA-beads complexes. Finally, the RNAs were eluted by wash

buffer and detected by qRT-PCR.

2.12. Immunoblotting assay

To perform the immunoblotting assay, all proteins were extracted using RIPA buffer supplemented with phosphatases and protease inhibitors (Bimake, #B15003 and #B14002). Proteins were quantified by BCA reagent (Yeasten, #20201ES90), separated by SDS-PAGE gel, and then transferred onto PVDF membranes. After blocking in 5 % Bovine Serum Albumin (BSA) (Proliant Biological, #69100) for 1 h, the membranes were incubated with indicated antibodies, including BTBD7 (Invitrogen, # PA5-45934), ROCK2 (CST, #47012), MMP-2 (CST, #40994), MMP-9 (CST, #13667), and GAPDH (CST, #5174) at 4 °C overnight. Following three washes in PBS, the membrane was treated with secondary antibodies. Finally, the signals were detected using an enhanced chemiluminescent (ECL) substrate kit (Yeasten, #36208ES80).

2.13. Tumor xenografts in nude mice

Animals were raised and handled following the procedures authorized by the Animal Experiment Committee of the *Affiliated Hangzhou First People's Hospital* and the institutional guidelines for the Care and Use of Laboratory Animals. To assess tumorigenesis ability, the reconstituted Hep3B cells were subcutaneously injected into the 6-week-old BALB/c nude mice. Tumor sizes were examined every week, and the growth index was calculated according to $0.5 \times \text{length} \times \text{width} \times \text{width}$. After five weeks, the tumors were harvested and weighed.

2.14. Statistics

Quantification and statistical analysis were carried out using SPSS software (version 23.0.), Image J (version 1.8.0), and GraphPad (version 8.0.2). All data were presented as mean \pm standard error (SD). The difference between two groups was calculated using two-tailed Student's *t*-test. $P < 0.05$ was considered as statistical significance (*, $P < 0.05$; **, $P < 0.01$; ***, $P < 0.001$; ns, no significance).

3. Results

3.1. CircZCCHC2 is upregulated in HCC and its overexpression predicts poor outcome of HCC patients

To explore potential circRNAs involved in HCC progression, we first analyzed the differentially expressed circRNAs from the circRNA expression data of six HCC patients deposited in the GEO dataset, GSE164803. We found that, among the top 20 highly expressed circRNAs, circZCCHC2 was remarkably overexpressed in HCC samples relative to the adjacent normal liver tissues (Fig. 1A and B). Fig. 1C shows that circZCCHC2 was derived from exons 2–5 of the maternal ZCCHC2 gene. Further, we assessed the expression levels of circZCCHC2 in the 60 pairs of HCC tissues and corresponding normal liver samples. As shown in Fig. 1D, circZCCHC2 was prominently elevated in HCC primary tumors in contrast to the matched normal tissues. Moreover, the expression level of circZCCHC2 was positively correlated to the stages of HCC (Fig. 1E). Next, we analyzed the survival of HCC patients and found that patients with higher expression levels of circZCCHC2 predicted shorter overall survival (Fig. 1F). Similarly, we observed that circZCCHC2 expression was elevated in the four HCC cell lines (Hep3B, HepG2, SK-HEP-1, and Huh7) relative to the normal hepatocyte line, LO2 (Fig. 1G).

Furthermore, to confirm the loop structure of circZCCHC2, the total RNAs extracted from Hep3B and HepG2 cells were treated with RNase R. QRT-PCR analysis revealed that circZCCHC2 was effectively resistant to degradation by RNase R compared to the mock group (negative control), whereas the linear ZCCHC2 mRNA did not (Fig. 1H). Moreover, we investigated the effect of actinomycin D on the expression of linear ZCCHC2 and circZCCHC2 in SW1990 cells. We observed that

actinomycin D significantly reduced linear ZCCHC2 expression in a time-dependent manner, while circZCCHC2 expression remained unchanged (Fig. 1I). Finally, to understand the subcellular location of circZCCHC2, we performed qRT-PCR and FISH assays and found that circZCCHC2 was localized in the cytoplasm (Fig. 1J and K). Together, these data confirm suggest that circZCCHC2 is located in the cytoplasm and is upregulated in HCC.

3.2. CircZCCHC2 knockdown inhibits HCC cell proliferation and metastasis abilities

To explore the biological function of circZCCHC2, we first knocked down circZCCHC2 (sh-circZCCHC2#1 and sh-circZCCHC2#2) in Hep3B and HepG2 cells by lentiviral infection. QRT-PCR analysis showed that endogenous circZCCHC2 expression was successfully inhibited in both sh-circZCCHC2#1 and sh-circZCCHC2#2 transfected cell lines (Fig. 2A). Cell growth curve and colony formation assays revealed that circZCCHC2 knockdown markedly attenuated the cell growth and colony capacities of Hep3B and HepG2 cells (Fig. 2B and C). Similarly, the EdU assay revealed that circZCCHC2 knockdown remarkably suppressed DNA replication activity, thus attenuating the cell proliferation ability of HCC cells (Fig. 2D). Since hepatocellular carcinoma is characterized by strong invasiveness and a high risk of distant metastasis, we then explored the effect of circZCCHC2 on the migratory and invasive ability of HCC cells. Knockdown of circZCCHC2 seriously reduced the potentials of migration and invasion of Hep3B and HepG2 cells (Fig. 2E and F). To explore the tumorigenic effect of circZCCHC2 *in vivo*, sh-NC and sh-circZCCHC2#1 expressing Hep3B cells were subcutaneously injected into nude mice. Consistent with the *in vitro* results, circZCCHC2 depletion led to significant inhibition of tumorigenesis (Fig. 2G–I). Together, these results confirm that circZCCHC2 contributes to the capacity for proliferation, migration, and invasion in HCC cells.

3.3. CircZCCHC2 acts as a sponge of miR-936

To further elucidate the molecular mechanism underlying the carcinogenic effect of circZCCHC2, we first determined whether circZCCHC2 sponged miRNA to regulate HCC progression. After a screening of the Circular RNA Interactome database, we found that miR-936 could be a target sponged by circZCCHC2 (Fig. 3A). To obtain molecular evidence of the direct interaction between circZCCHC2 and miR-936, we carried out the dual luciferase reporter assay, finding that miR-936 overexpression reduced the luciferase activity in Hep3B and HepG2 cells co-transfected with circZCCHC2 wild-type but not in the cells co-transfected with circZCCHC2 mutant (Fig. 3B). Similarly, the RNA-RNA pulldown assay revealed that miR-936 was highly enriched by the bio-circZCCHC2 relative to the non-specific bio-NC (Fig. 3C). These data imply that circZCCHC2 can directly bind to miR-936 through complementary sequences. Subsequently, we examined miR-936 expression levels in four HCC cell lines (Hep3B, SK-HEP-1, HepG2, and Huh7) and a normal hepatocyte line (LO2).

As shown in Fig. 3D, miR-936 was generally downregulated in all HCC cell lines relative to the normal control. As miR-936 is known to function as a tumor-suppressing gene in various human cancers [14,15], we then examined miR-936 expression in 60 pairs of HCC tissues and adjacent healthy tissues, suggesting that miR-936 was obviously decreased in HCC tissues relative to normal liver tissues (Fig. 3E). Additionally, spearman analysis implied that the expression levels of miR-936 was negatively correlated with that of circZCCHC2 (Fig. 3F). We further examined whether circZCCHC2 exerted a carcinogenic effect on HCC progression by regulating miR-936. The results of qRT-PCR demonstrated that miR-936 expression was elevated by circZCCHC2 knockdown, while reduced by co-transfection with miR-936 inhibitors (Fig. 3G). Moreover, the cell growth curve showed that the suppressed cell proliferation mediated by circZCCHC2 knockdown in Hep3B and HepG2 cells could be reversed by co-transfected with miR-936 inhibitors

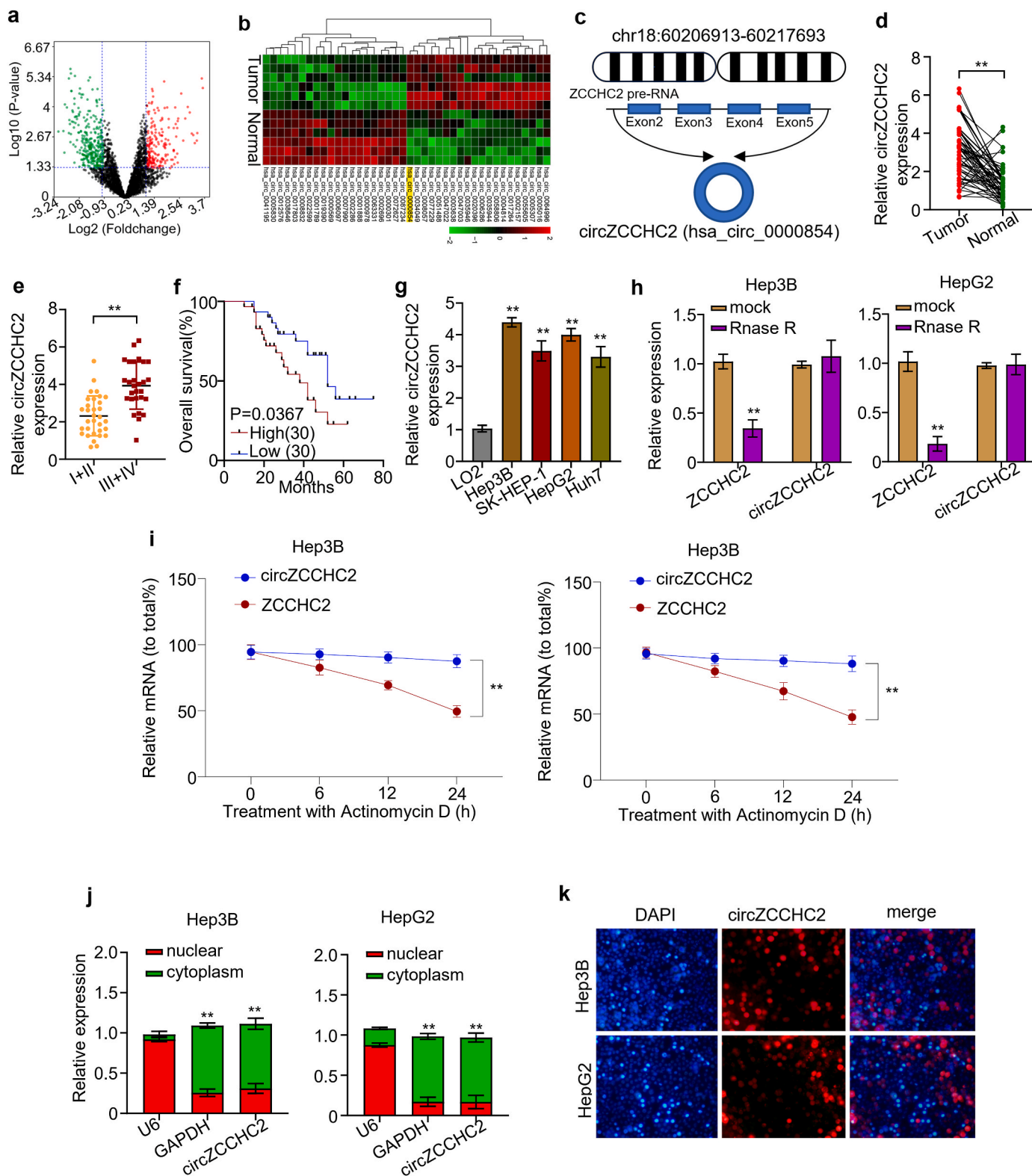


Fig. 1. CircZCCHC2 is upregulated in PC and its overexpression predicts poor outcome of HCC patients. (A–B). Volcano plot (A) and heatmap (B) analysis of the differentially expressed circRNAs between HCC tissues and adjacent normal tissues according to the GEO database, GES164803. (C). Schematic illustration of the formation of circZCCHC2 through backing splicing of exon 2–5 of ZCCHC2. (D). Detection of circZCCHC2 expression levels in 60 pairs of HCC and adjacent normal tissues by qRT-PCR. (E). Analysis of circZCCHC2 expression in HCC patients of different clinical stages. (F). Kaplan-Meier curves for overall survival of HCC patients with low or high expression of circZCCHC2. (G). QRT-PCR analysis of circZCCHC2 expression in a normal hepatocyte line (LO2) and four HCC cell lines (Hep3B, SK-HEP-1, HepG2, and Huh7). (H). QRT-PCR analysis of circZCCHC2 expression in Hep3B and HepG2 cells treated with RNase R compared to the mock group (negative control). (I). The levels of ZCCHC2 linear mRNA and circZCCHC2 were detected by RT-qPCR in HCC cells treated with Actinomycin D for 0, 6, 12, and 24 h. (J). QRT-PCR analysis of the relative expression levels of circZCCHC2 in nuclear and cytoplasm of Hep3B and HepG2 cells. (K). FISH assay determining the subcellular location of circZCCHC2.

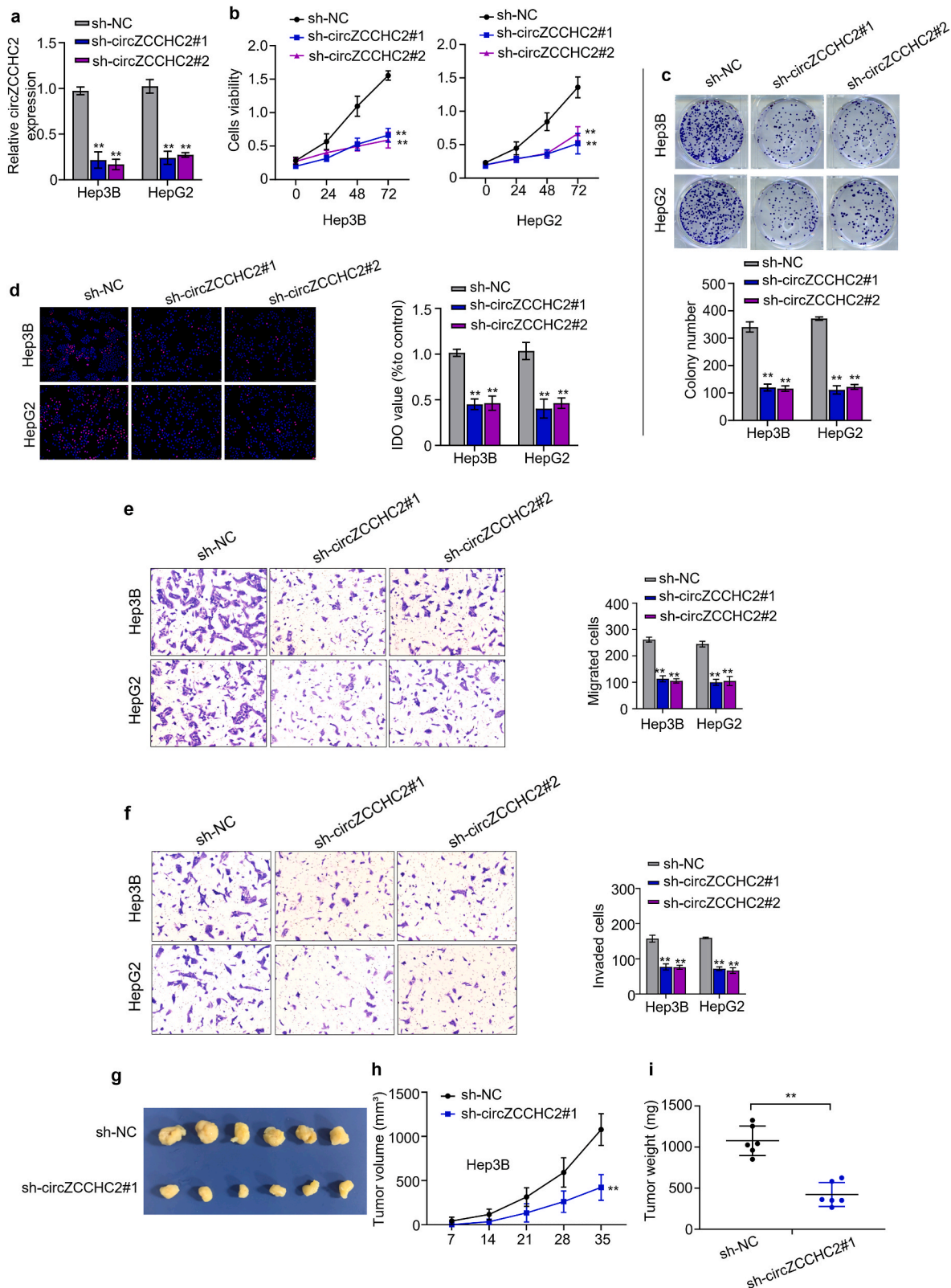


Fig. 2. CircZCCHC2 promotes the cell proliferation and invasiveness in HCC. (A). QRT-PCR analysis confirming the establishment of Hep3B and HepG2 cells stably expressing shNC or sh-circZCCHC2 (#1 and #2) by lentiviral infection. (B–C). CCK-8 (B) and colony formation (C) assay examining the proliferation of Hep3B and HepG2 cells stably expressing sh-NC and sh-circZCCHC2 (#1 and #2). (D). EdU detection assay assessing the proliferation of Hep3B and HepG2 cells transfected with shNC or two different shRNA targeting circZCCHC2. (E–F). Boyden's chamber migration (E) and Matrigel-coated invasion (F) assays detecting the invasiveness of Hep3B and HepG2 cells stably expressing shNC and sh-circZCCHC2 (#1 and #2). (G). Representative images showing the xenograft tumors generated by subcutaneous inoculation of shNC- and sh-circZCCHC2-expressing Hep3B cells into 6-week-old female BALB/c nude mice (n = 6). After 6 weeks of inoculation, xenograft tumors were harvested. Photographs of tumors (G), (H). Growth curve of tumor volumes. (I). Weight of xenograft tumors.

(Fig. 3H). Similarly, the inhibited potentials of migration and invasion of Hep3B and HepG2 cells caused by circZCCHC2 knockdown were obviously restored after miR-936 inhibition (Fig. 3I and J). The above results suggest that circZCCHC2 promotes HCC growth and metastasis by regulating miR-936.

3.4. CircZCCHC2 regulates BTBD7 expression by sponging miR-936 in HCC cells

A prediction by miRDB revealed that there were complementary sequences between miR-936 and BTBD7 (Fig. 4A). To further verify the above hypothesis, we firstly performed the dual luciferase reporter assay, exhibiting that ectopic expression of miR-936 robustly attenuated the luciferase activity of Hep3B and HepG2 cells co-transfected with BTBD7 wild-type, while having little if any, effect on the luciferase activity in Hep3B and HepG2 cells co-transfected with mutant BTBD7 vectors (Fig. 4B). Moreover, the result of the RNA-RNA pulldown assay exhibited that both the miR-936 and BTBD7 expression levels were heightened by the anti-Ago2 antibody compared with the IgG antibody, suggesting a binding between miR-936 and BTBD7 (Fig. 4C). In addition, BTBD7 expression was decreased by miR-936 overexpression, while increased by miR-936 downregulation in Hep3B and HepG2 cells (Fig. 4D). Meanwhile, both mRNA and protein of BTBD7 were consistently elevated in HCC samples by relative to normal tissues (Fig. 4E and F). These results suggest that miR-936 targets BTBD7 and decreases its expression to suppress progression.

3.5. CircZCCHC2 accelerates HCC progression via regulating miR-936/BTBD7 axis and activating Rho/ROCK2 pathway

Considering the evidence showing that circZCCHC2 sponges miR-936 and miR-936 directly targets BTBD7, we reasoned that circZCCHC2 can regulate BTBD7 expression levels by sponging miR-936. To verify this assumption, the HCC cells were transfected with sh-NC, sh-circZCCHC2#1, sh-circZCCHC2#1+anti-miR-NC, and sh-circZCCHC2#1+anti-miR-936, respectively. The mRNA expression levels of BTBD7 were decreased by circZCCHC2 knockdown, while the effect was reversed in Hep3B and HepG2 cells after co-transfection with anti-miR-936 (Fig. 5A), indicating that circZCCHC2 contributed to HCC deterioration through modulating miR-936/BTBD7 axis. Given that BTBD7/ROCK2 signaling pathway plays a crucial function in the tumorigenesis and progression of HCC [16,17], we further investigated whether circZCCHC2 regulates HCC progression by regulating the miR-936/BTBD7/ROCK2 pathway. As shown in Fig. 5B, the expression levels of BTBD7 and the downstream signal molecules, such as ROCK2, MMP-2 and MMP-9, were inhibited by circZCCHC2 knockdown, while increased by co-transfection with anti-miR-936. Collectively, these experiments clarify that circZCCHC2 accelerates HCC progression via modulating the miR-936/BTBD7/ROCK2 signaling pathway (Fig. 5C).

4. Discussion

HCC is categorized as the most aggressive and refractory primary liver cancer characterized by extremely high mortality. Therefore, elucidation of the mechanism of HCC development and progression, and identification of new therapeutic targets have received much research attention. Recently, it has been reported that circRNAs play critical roles

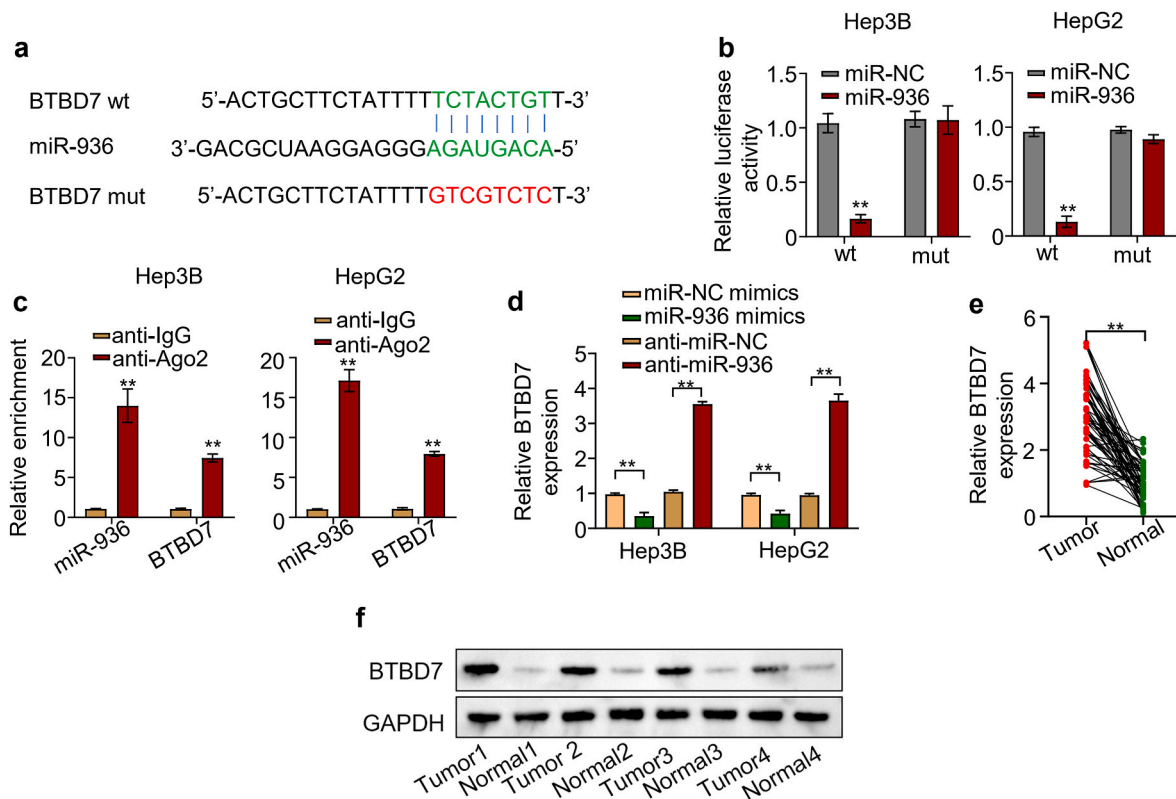


Fig. 4. CircZCCHC2 regulates BTBD7 expression by sponging miR-936 in HCC cells. (A). Complementary sites between miR-936 and BTBD7 predicted by the miRDB. (B). Luciferase activity of Hep3B and HepG2 cells co-transfected with NC or miR-936 mimics together with BTBD7 wild-type or mutant. (C). Enrichment of miR-936 and BTBD7 by anti-Ago2 antibody. (D). QRT-PCR analysis of BTBD7 expression in Hep3B and HepG2 cells co-transfected with NC or miR-936 mimics together with anti-NC or anti-miR-936. (E). Detection of BTBD7 expression levels in 60 pairs of HCC and adjacent normal tissues by qRT-PCR. (F). Analysis of BTBD7 expression levels in four pairs of HCC and adjacent normal tissues by Western blot.

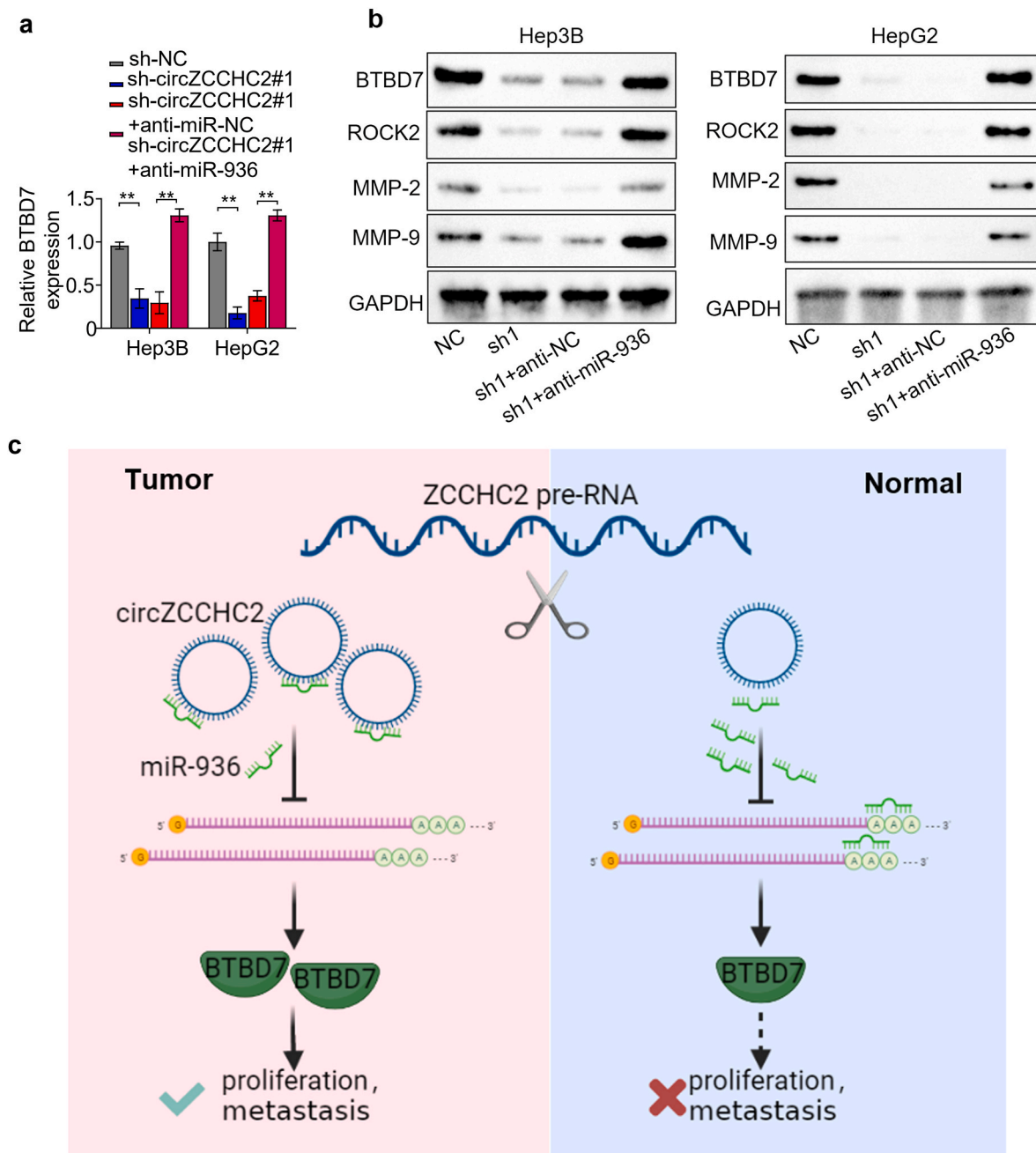


Fig. 5. CircZCCHC2 promotes HCC progression through modulating the miR-936/BTBD7 axis and activating the Rho/ROCK2 pathway. (A). QRT-PCR analysis of BTBD7 expression in Hep3B and HepG2 cells co-transfected with shNC or shcircZCCHC2 along with *anti*-NC or *anti*-miR-936. (B). Immunoblot detecting BTBD7, ROCK2, MMP-2 and MMP-9 in Hep3B and HepG2 cells co-transfected with shNC or shcircZCCHC2 along with *anti*-NC or *anti*-miR-936. (C). A model recapitulating the action mode of circZCCHC2 in HCC development and progression. In normal cells, circZCCHC2 expression level is low and does not play important roles in cell growth (Right). In HCC, circZCCHC2 is formed by the back splicing of ZCCHC2 pre-RNA (Left), which results in the upregulation of circZCCHC2 that facilitates HCC progression by regulating the miR-936/BTBD7 axis.

in HCC development and progression. Some circRNAs promote the malignancy of HCC, such as circ-DB [18], circRHOT1 [19], and circ_MMP2 [20], while some circRNAs such as hsa_circ_0110102 [21] and hsa_circ_103809, inhibit HCC tumorigenesis and progression [22]. In this report, we identified that circZCCHC2 was highly expressed in HCC and functioned as a tumor promoter, which accelerated the tumor growth and metastasis of HCC cells and is negatively correlated with the prognosis. In general, circRNAs regulate cell activities by sponging miRNAs. For example, circ_0005909 and circ_0001162 sponge miR-936 to regulate the expression levels of HMGB1 and ERBB4 in osteosarcoma and glioma, respectively [23,24]. In the current study, our results

revealed that circZCCHC2 sponges miR-936 to facilitate HCC progression. In addition, we observed that miR-936 is downregulated in HCC tissues, which is consistent with a previous study [25]. Moreover, miR-936 has been reported to function as a tumor suppressor in many tumor types, such as laryngeal squamous cell carcinoma [14], gastric cancer [15], and non-small cell lung cancer [26]. Consistently, our study showed that the downregulation of miR-936 by circZCCHC2 facilitates the proliferation and invasiveness of HCC cells, and these data indicated that miR-936 also functions as a tumor suppressor in HCC.

Typically, miRNAs bind to downstream target mRNAs and consequently inhibit their expression [27]. For example, miR-936 directly

targets HDAC9 to inactivate the PI3K/AKT pathway, thereby inhibiting the malignant phenotype of retinoblastoma [28]. In ovarian cancer, miR-936 was proved to target the FGF2 gene [29]. Our results illustrated that miR-936 directly binds to BTBD7. BTBD7, a branching morphogenesis-associated gene, plays significant roles in the process of epithelial-mesenchymal transition (EMT) in human malignancies, such as lung cancer [30,31] and salivary adenoid cystic carcinoma [32]. Moreover, it has been reported that BTBD7 accelerates angiogenesis and metastasis of HCC through regulating the EMT process and activating the RhoC-Rock2 signaling pathway [16,17]. Intriguingly, our rescue experiments showed that the suppressed BTBD7/ROCK2 signaling pathway caused by circZCCHC2 knockdown could be effectively reactivated by miR-936 inhibition. Collectively, we conclude that circZCCHC2 sponges miR-936 to regulate the BTBD7/ROCK2 pathway, promoting HCC development and progression.

In sum, our study first elucidated a novel discovering circRNA named circZCCHC2, which was significantly elevated in HCC tissues and predict the poor prognosis. Our results investigated the significant roles of circZCCHC2 in HCC and reported that circZCCHC2 promoted HCC progression by regulating the miR-936/BTBD7 axis and activating the Rho/ROCK2 signaling pathway, which providing a new strategy for early diagnosis and therapeutic for HCC patients.

Ethics approval and consent to participate

This study was approved by an institutional review board of the Affiliated Hangzhou First People's Hospital, and written informed consent was obtained from all participants.

Consent for publication

All patients in this study provided their consent for publication.

Availability of data and materials

The datasets used and/or analyzed during the current study are available from the corresponding author on reasonable request.

Funding

No funding.

CRedit authorship contribution statement

Junjie Yin: Conceptualization, Data curation, Project administration, Writing – original draft. **Mian Wang:** Conceptualization, Investigation, Methodology, Writing – original draft. **Jian Chen:** Data curation, Investigation. **Huigang Li:** Investigation, Software. **Jianyong Zhuo:** Software, Supervision, Validation. **Bei Lu:** Data curation, Visualization. **Yang Cai:** Conceptualization, Project administration, Writing – review & editing.

Declaration of competing interest

The authors declare that they have no known competing financial interests or personal relationships that could have appeared to influence the work reported in this paper.

Acknowledgement

Not applicable.

References

- [1] T.K.-W. Lee, X.-Y. Guan, S. Ma, Cancer stem cells in hepatocellular carcinoma - from origin to clinical implications, *Nat. Rev. Gastroenterol. Hepatol.* 19 (1) (2022) 26–44.
- [2] H. Sung, J. Ferlay, R.L. Siegel, et al., Global cancer statistics 2020: GLOBOCAN estimates of incidence and mortality worldwide for 36 cancers in 185 countries, *Cancer J. Clin.* 71 (3) (2021) 209–249.
- [3] H.B. El-Serag, Epidemiology of viral hepatitis and hepatocellular carcinoma, *Gastroenterology* 142 (6) (2012).
- [4] J.D. Yang, P. Hainaut, G.J. Gores, et al., A global view of hepatocellular carcinoma: trends, risk, prevention and management, *Nat. Rev. Gastroenterol. Hepatol.* 16 (10) (2019) 589–604.
- [5] S. D'Souza, K.C. Lau, C.S. Coffin, et al., Molecular mechanisms of viral hepatitis induced hepatocellular carcinoma, *World J. Gastroenterol.* 26 (38) (2020) 5759–5783.
- [6] F. Wei, Neoadjuvant immunotherapy for resectable hepatocellular carcinoma, *Lancet Gastroenterol Hepatol* 7 (6) (2022) 504.
- [7] J. Xu, L. Ji, Y. Liang, et al., CircRNA-SORE mediates sorafenib resistance in hepatocellular carcinoma by stabilizing YBX1, *Signal Transduct. Targeted Ther.* 5 (1) (2020) 298.
- [8] X.-Y. Huang, Z.-L. Huang, J. Huang, et al., Exosomal circRNA-100338 promotes hepatocellular carcinoma metastasis via enhancing invasiveness and angiogenesis, *J. Exp. Clin. Cancer Res. : CR* 39 (1) (2020) 20.
- [9] G. Huang, M. Liang, H. Liu, et al., CircRNA hsa_circRNA_104348 promotes hepatocellular carcinoma progression through modulating miR-187-3p/RTKN2 axis and activating Wnt/ β -catenin pathway, *Cell Death Dis.* 11 (12) (2020) 1065.
- [10] Z. Liu, Y. Yu, Z. Huang, et al., CircRNA-5692 inhibits the progression of hepatocellular carcinoma by sponging miR-328-5p to enhance DAB2IP expression, *Cell Death Dis.* 10 (12) (2019) 900.
- [11] D.-D. Xiong, Y.-W. Dang, P. Lin, et al., A circRNA-miRNA-mRNA network identification for exploring underlying pathogenesis and therapy strategy of hepatocellular carcinoma, *J. Transl. Med.* 16 (1) (2018) 220.
- [12] X.-Y. Huang, P.-F. Zhang, C.-Y. Wei, et al., Circular RNA circMET drives immunosuppression and anti-PD1 therapy resistance in hepatocellular carcinoma via the miR-30-5p/snail/DPP4 axis, *Mol. Cancer* 19 (1) (2020) 92.
- [13] J. Yu, Q.-G. Xu, Z.-G. Wang, et al., Circular RNA cSMARCA5 inhibits growth and metastasis in hepatocellular carcinoma, *J. Hepatol.* 68 (6) (2018) 1214–1227.
- [14] X.-J. Lin, H. Liu, P. Li, et al., miR-936 suppresses cell proliferation, invasion, and drug resistance of laryngeal squamous cell carcinoma and targets GPR78, *Front. Oncol.* 10 (2020) 60.
- [15] S. Liu, Y. Gong, X.-D. Xu, et al., MicroRNA-936/ERBB4/Akt axis exhibits anticancer properties of gastric cancer through inhibition of cell proliferation, migration, and invasion, *Kaohsiung J. Med. Sci.* 37 (2) (2021) 111–120.
- [16] Y.-M. Tao, J.-L. Huang, S. Zeng, et al., BTB/POZ domain-containing protein 7: epithelial-mesenchymal transition promoter and prognostic biomarker of hepatocellular carcinoma, *Hepatology* 57 (6) (2013) 2326–2337.
- [17] K. Hu, Z. Wang, Y. Tao, Suppression of hepatocellular carcinoma invasion and metastasis by Rho-kinase inhibitor Fasudil through inhibition of BTBD7-ROCK2 signaling pathway, *Zhong Nan Da Xue Xue Bao Yi Xue Ban = J. Central South Univ. Med. Sci.* 39 (12) (2014) 1221–1227.
- [18] H. Zhang, T. Deng, S. Ge, et al., Exosome circRNA secreted from adipocytes promotes the growth of hepatocellular carcinoma by targeting deubiquitination-related USP7, *Oncogene* 38 (15) (2019) 2844–2859.
- [19] L. Wang, H. Long, Q. Zheng, et al., Circular RNA circRHOT1 promotes hepatocellular carcinoma progression by initiation of NR2F6 expression, *Mol. Cancer* 18 (1) (2019) 119.
- [20] D. Liu, H. Kang, M. Gao, et al., Exosome-transmitted circ MMP2 promotes hepatocellular carcinoma metastasis by upregulating MMP2, *Mol. Oncol.* 14 (6) (2020) 1365–1380.
- [21] X. Wang, W. Sheng, T. Xu, et al., CircRNA hsa_circ_0110102 inhibited macrophage activation and hepatocellular carcinoma progression via miR-580-5p/PPAR α /CCL2 pathway, *Aging* 13 (8) (2021) 11969–11987.
- [22] X. Li, M. Shen, Circular RNA hsa_circ_103809 suppresses hepatocellular carcinoma proliferation and invasion by sponging miR-620, *Eur. Rev. Med. Pharmacol. Sci.* 23 (2) (2019) 555–566.
- [23] S. Ding, G. Zhang, Y. Gao, et al., Circular RNA hsa_circ_0005909 modulates osteosarcoma progression via the miR-936/HMGB1 axis, *Cancer Cell Int.* 20 (2020) 305.
- [24] D. Zhou, X. Lin, P. Wang, et al., Circular RNA circ_0001162 promotes cell proliferation and invasion of glioma via the miR-936/ERBB4 axis, *Bioengineered* 12 (1) (2021) 2106–2118.
- [25] J. Tian, Y. Zhao, L. Li, et al., MicroRNA-936 targets JAG1 and inhibits the proliferation of hepatocellular carcinoma cells, *Technol. Cancer Res. Treat.* 20 (2021) 1533033820985785.
- [26] X. Zhou, H. Tao, Overexpression of microRNA-936 suppresses non-small cell lung cancer cell proliferation and invasion via targeting E2F2, *Exp. Ther. Med.* 16 (3) (2018) 2696–2702.
- [27] Z. Jia, J. An, Z. Liu, et al., Non-coding RNAs in colorectal cancer: their functions and mechanisms, *Front. Oncol.* 12 (2022) 783079.
- [28] L. Xu, W. Li, Q. Shi, et al., MicroRNA-936 inhibits the malignant phenotype of retinoblastoma by directly targeting HDAC9 and deactivating the PI3K/AKT pathway, *Oncol. Rep.* 43 (2) (2020) 635–645.
- [29] C. Li, S. Yu, S. Wu, et al., MicroRNA-936 targets FGF2 to inhibit epithelial ovarian cancer aggressiveness by deactivating the PI3K/Akt pathway, *OncoTargets Ther.* 12 (2019) 5311–5322.

- [30] J. Shu, L. Wang, F. Han, et al., BTBD7 downregulates E-cadherin and promotes epithelial-mesenchymal transition in lung cancer, *BioMed Res. Int.* 2019 (2019) 5937635.
- [31] C. Fan, Y. Miao, X. Zhang, et al., Btd7 contributes to reduced E-cadherin expression and predicts poor prognosis in non-small cell lung cancer, *BMC Cancer* 14 (2014) 704.
- [32] L. Yang, T. Wang, J. Zhang, et al., BTBD7 silencing inhibited epithelial-mesenchymal transition (EMT) via regulating Slug expression in human salivary adenoid cystic carcinoma, *Cancer Biomarkers : Section A of Disease Markers* 20 (4) (2017) 461–468.